The Competitive Binding of Proteins to Gold Nanoparticles Disclosed by Molecular Dynamics Simulations

ARTICLE *in* THE JOURNAL OF PHYSICAL CHEMISTRY C · SEPTEMBER 2015

Impact Factor: 4.77 · DOI: 10.1021/acs.jpcc.5b05796

3 AUTHORS:

Francesco Tavanti
Università degli Studi di Modena e Reggio Emilia
5 PUBLICATIONS **7** CITATIONS
SEE PROFILE

Alfonso Pedone
Università degli Studi di Modena e Reggio Emilia
87 PUBLICATIONS **1,449** CITATIONS
SEE PROFILE

Maria Cristina Menziani
Università degli Studi di Modena e Reggio Emilia
166 PUBLICATIONS **2,702** CITATIONS
SEE PROFILE

THE JOURNAL OF PHYSICAL CHEMISTRY C

Article

pubs.acs.org/JPCC

Competitive Binding of Proteins to Gold Nanoparticles Disclosed by Molecular Dynamics Simulations

Francesco Tavanti, Alfonso Pedone, and Maria Cristina Menziani*

Dipartimento di Scienze Chimiche e Geologiche, Università di Modena e Reggio Emilia, Via G. Campi 103, 41125 Modena, Italy

Supporting Information

ABSTRACT: This work reports the results of coarse-grained molecular dynamics simulations of citrate-coated gold nanoparticles (AuNPs) in interaction with insulin and fibrinogen, two of the most abundant proteins in the plasma. The following have been found: (a) The corona of citrate-coated AuNP of 5 nm core diameter is composed by a single layer of proteins comprising a maximum of 20 insulins, whereas only 3 fibrinogens are contemporaneously present. (b) The binding site for insulin is specific and independent from the number of insulins considered in the computational simulations, whereas fibrinogen presents different binding modes, as a function of protein concentration and composition. Moreover, fibrinogen is able to accommodate two citrate-coated AuNPs in independent binding sites localized at the ending nodes. (c) A competitve process for AuNP binding is observed when insulins and fibrinogens are contemporaneously present in the simulations. (d) The overall protein secondary structure is maintained upon binding to a single citrate-coated AuNP, but small changes in helix and sheet percentages are observed for both proteins. (e) A partial unfolding of the α-helix bundle is found for fibrinogen bound to two AuNPs. This may provide a molecular level understanding of the inflammatory response to nanoparticles.

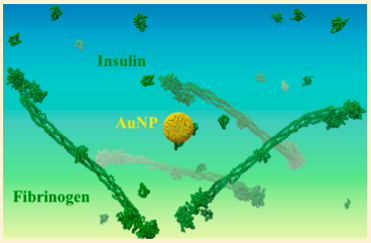

INTRODUCTION

In the last years, the interest in the interaction of nanoparticles (NPs) with biological medium is grown due to the huge number of possible applications in nanomedicine and nanotechnology.[1,2] It is well-known that the contact between NPs and biological medium triggers a competition between different biological molecules to adsorb on the surface of the nanoparticles.[3]

The composition of the protein corona is unique to each NP,[4] and mediates the interaction of the NP with biological machineries, eliciting the physiological response (i.e., agglomeration, cellular uptake, circulation lifetime, signaling, kinetics, transport, accumulation, and toxicity).[5,6]

The mechanism of formation of the protein corona is still poorly understood,[2,6−9] being a complex process that depends on many parameters, such as the physicochemical properties of the NP (size, shape, composition, surface decoration, and surface charges), the nature of the physiological environment (blood, cell cytoplasm, etc.), and the duration of exposure.

Moreover, the effect of the physicochemical properties of the NP on the native structure of the absorbed protein has been demonstrated as being potentially responsible for abnormal functions coming to diseases.[10−12]

Precious information on these processes can be gained by computer simulations techniques, which proved to be of tremendous help to understand the structure and dynamics of biological macromolecules in different environments.[2,6,13,14]

In this work, coarse-grained molecular dynamics simulations of citrate-coated gold nanoparticles (AuNPs) in interaction with insulin and fibrinogen will be carried out. These two proteins are among the most abundant in the plasma and show very different physicochemical properties, and their abnormal conformational changes could promote autoimmune diseases and inflammation.[15−18]

To our knowledge, this is the first computational study that addresses the effect of protein concentration, protein competition, and multiple nanoparticles on the interaction of two important plasma proteins with AuNPs. To validate the computational results, a wide comparison with the experimental data available in the literature on these or similar systems will be carried out.[16,18−20] Moreover, potential biological and toxicological implications will also be discussed.

METHODS

Coarse-Grained Model. The AuNP of 5 nm diameter was built using a coarse-grained model previously described,[13] and summarized as follows: (1) 48 positively charged beads (+e) were randomly placed on a spherical surface at 2.5 nm from the center of the NP, maintaining a uniform distribution of beads.[21,22] On the center of the bead distribution, a neutral bead associated with a repulsive spherical wall provides a spherical shape to the AuNP and avoids the penetration of citrates and proteins throughout the AuNP surface. (2) 100 beads with negative charge (−3e) representing citrate molecules were randomly distributed in the AuNP surroundings. (3) A 100 ns molecular dynamics simulation was performed on a simplified system formed by the AuNP and 100 citrates in order to determine the maximum number of

Received: June 17, 2015
Revised: September 8, 2015
Published: September 8, 2015

DOI: 10.1021/acs.jpcc.5b05796
J. Phys. Chem. C 2015, 119, 22172−22180

citrates adsorbed on the AuNP surface. It was observed that, in the interval between 80 and 100 ns, 37 citrates remain constantly bound on the AuNP, and no additional citrates are adsorbed on the AuNP surface. (4) The last simulation frame was used as input for the protein-AuNP simulations, after deletion of unbound citrates. The extended diameter of the AuNP after citrate-coating is 5.7 nm. The overall negative charge of the resulting citrate-coated AuNP is in agreement with experimental measurements of the ζ-potential of similar systems.[18]

The crystal structures of fibrinogen and insulin were retrieved from the Protein Data Bank (PDB): the fibrinogen 3GHG[23] and insulin 4EWZ[24] structures were chosen as they show the best resolution and the highest homology with the wild-type structure among all the structures deposited in the PDB.

The proteins were treated with a CG single-bead model: Each amino acid was replaced by a single bead with the same mass and total charge of the related amino acid and with the same coordinates of the α-carbon atom. The approach used was necessary to reduce the high computational cost given by the number of proteins involved, and to maintain a good spatial and temporal resolution.[25−28]

The standard protonation states at pH 7 were assigned to the treatable amino acid residues of the proteins.

Force Field. The force field used to model protein−AuNP interactions[13] is briefly summarized:

$$U = \sum U_{\text{bonded}} + \sum U_{\text{nonbonded}} \tag{1}$$

where

$$\sum U_{\text{bonded}} = \sum_{i,j} U_{\text{bonds}}(i, j) + \sum_{i,j,k} U_{\text{angles}}(i, j, k) + \sum_{i,j,k,l} U_{\text{dihedrals}}(i, j, k, l) \tag{2}$$

$$\sum U_{\text{nonbonded}} = \sum_{i,j} U^{\text{local}}_{\text{nonbonded}}(i, j) + \sum_{i,j} U^{\text{nonlocal}}_{\text{nonbonded}}(i, j) \tag{3}$$

The functional form of the force field comprises a short-term potential (U_{bonded}) and a long-term potential ($U_{\text{nonbonded}}$). The first term describes bonds, angles, and dihedrals of proteins. Parameters related to these potentials (R, θ_0, and φ_0) are calculated on the reference structure of proteins. Force field parameters for proteins are reported in refs 26−28. Citrate force field parameters are adapted from Ding et al.[29] All parameters are described in Table S.1 in the Supporting Information.

Nonlocal nonbonded interactions describe van der Waals and electrostatic potentials established between the AuNP and the protein and among protein beads. Protein beads that are closer to the cutoff of 8.5 Å interact through nonbonded local terms, while beads beyond the cutoff interact with nonlocal nonbonded terms. The cutoff for the nonlocal nonbonded terms is set to 30 Å in order to take into account interactions with the repulsive spherical wall of the central gold bead.

Protein−AuNP and citrate−AuNP interactions are accounted for by van der Waals and electrostatic terms described by Li et al.[30] VdW interactions describe excluded volume interactions between two beads with distance r_{ij}

$$U_{\text{VdW}} = \sum_{i,j} \left(\frac{\sigma}{r_{ij}}\right)^{12} \tag{4}$$

where σ is the reference radius set to 3.8 Å.

Electrostatic interactions between two beads of charge z_i and z_j at a distance r_{ij} are given by the Debye−Hückel potential

$$U_{\text{elec}} = \sum_{i,j} \frac{z_i z_j e^2}{4\pi\varepsilon_0\varepsilon_r\varepsilon_{ij}} e^{-r_{ij}/l_D} \tag{5}$$

where l_D is the Debye length defined as $l_D = (8\pi l_b I)^{1/2}$ and l_b is the Bjerrun length at room temperature which is set to 7 Å. The ionic strength (I) is set to an ion concentration of 150 mM, and the dielectric constant, ε, is set to 10 to maximize the speed of the corona formation process and to avoid very long computational times.

It is generally assumed that for a citrate-capped nanoparticle electrostatic interaction plays an important role in NP−protein interaction at initial stages of the protein corona formation.[31,32] Thus, notwithstanding the significant approximations made in codifying the attracting forces, this force field was shown to be able to represent the corona formation in reasonable agreement with the available experimental data.[13,30,31]

Molecular Dynamics. Molecular dynamics simulations were performed using the DL_POLY_2.20 software.[33] The temperature of the system was maintained constant at 300 K using the Berendsen thermostat. The time-step used was 1 fs, and each trajectory was 50 ns long; this was the time required to reach a stable number of proteins adsorbed on the AuNP surface. Because of the approximations that were done, the length of the trajectory has not to be intended as the effective corona formation time scale; the accelerated dynamics of the system is necessary to simulate a process, which involves dozens of proteins, and evolves in a macroscopic time scale.

Three independent simulations have been performed for each system by changing the initial starting velocities in order to increase the statistics of the production runs.

Two kinds of simulations were performed: (1) The two systems AuNP-insulins and AuNP-fibrinogens were simulated separately by changing the number of proteins in the simulations in order to study the effect of protein concentration on the maximum number of adsorbed proteins. Simulations were performed with 10, 20, 34, 50, 70, and 100 insulin proteins and with 1, 2, 4, and 8 fibrinogen proteins. The AuNP was fixed at the center of a cubic box with boundary periodic conditions. The citrate molecules were free to move. (2) To observe the competitive binding of the two proteins, computational simulations at different insulin/fibrinogen ratio (10:1, 20:2, 34:4) were carried out.

Electrostatic Potential Surfaces. The electrostatic potential surfaces of insulin and fibrinogen are calculated using the built-in plugin of the Swiss-Pdb Viewer[34] using the same parameters as used in molecular dynamics simulations, that is, a ionic strength I of 150 mM and a dielectric constant ε of 10.

Contact Probability between Proteins and Citrate-Coated AuNP. The contact probability for each amino acid residue is defined as the ratio of the amount of time in which the distance of a given amino acid residue of the protein X from the NP surface is less than a given cutoff (6.5 Å), and the amount of time in which the protein X remains adsorbed on

DOI: 10.1021/acs.jpcc.5b05796
J. Phys. Chem. C 2015, 119, 22172−22180

the NP surface. These values are normalized in order to obtain the sum of all probabilities equal to 1.[13]

Insulins are considered adsorbed on the AuNP if the distance between the center of mass of the protein and the AuNP surface is closer than 19 Å. This value is estimated by considering the center of mass of insulin at 10 Å from its surface plus a bonding distance of 9 Å in order to take into account insulins bonded to citrates on the AuNP surface besides the insulins directly adsorbed on the AuNP surface. The shape and compact structure of this protein justify this approximation.

Due to its elongated shape, the procedure described above is not suitable for fibrinogen. In this case, the number of fibrinogens bound to the AuNP are simply counted by visualization of the trajectory of the simulations using the VMD software.[35]

Protein Conformational Changes. Atomistic representations of each coarse-grained protein were remapped using the MaxSprout Web server.[36] The backbone dihedral angles of each reconstructed structure were calculated using the built-in Ramachandran plot tool.[34]

Conformational changes of the protein upon binding to the citrate-coated AuNP were computed on the last configuration reached by each adsorbed protein. Free proteins were not used for calculations.

Protein Binding Energy. The total energy of the systems considered can be defined as follows:

$$E_{\text{tot}} = E_{\text{citrates-AuNP}} + \sum_n E_{\text{prot}} + E_{\text{interaction}} \tag{6}$$

Here $E_{\text{citrates-AuNP}}$ is the total energy of the citrate-coated AuNP, and $\sum_n E_{\text{prot}}$ is the summation over the internal energy of all proteins in the system. Moreover

$$E_{\text{interaction}} = E^{\text{interaction}}_{\text{prot-prot}} + E^{\text{all}}_{\text{binding}} \tag{7}$$

where $E^{\text{interaction}}_{\text{prot-prot}}$ refers to the interaction energy among all the proteins in the simulation box, and $E^{\text{all}}_{\text{binding}}$ is the binding energy of the adsorbed proteins with the citrate-coated AuNP. By replacing the interaction energy term, $E_{\text{interaction}}$, in eq 6, and simplifying

$$E^{\text{all}}_{\text{binding}} = E_{\text{tot}} - E_{\text{citrates-AuNP}} - \sum_n E_{\text{prot}} - E^{\text{interaction}}_{\text{prot-prot}} \tag{8}$$

The summation of the total internal energy of proteins and the interaction energy between proteins are calculated as the total energy of all proteins, $E^{\text{total}}_{\text{prot}}$.

All energy terms were obtained by averaging four energy minimized configurations sampled at 42, 45, 48, and 50 ns, when the maximum number of adsorbed proteins is reached. A 100 step minimization procedure was performed for each selected configuration before energy computation in order to remove unphysical contacts without changing significantly the system conformation.

The binding energy for each protein, E_{binding}, is obtained by dividing the overall binding energy, $E^{\text{all}}_{\text{binding}}$, by the number of adsorbed proteins in each simulation.

It is worth underlining that although the maximum adsorption capacity for the computational simulation with 10 insulins is six, the calculation of E_{binding} has been performed by sampling configurations containing only four adsorbed proteins on the AuNP, since the last two insulins adsorb only in the late stage of the computational simulations.

Interaction of Fibrinogen with Two AuNPs. The interaction of a single fibrinogen molecule with two AuNPs has also been investigated. In this case, one molecule of fibrinogen was positioned in a cubic box with two citrate-coated AuNPs having a gold core of 5 nm diameter (extended-diameter, after citrates coating: 5.7 nm) positioned at approximately 30 nm from its center of mass. In order to explore multiple configurations the fibrinogen and the two citrate-coated AuNPs were allowed to move freely.

Harmonic potentials with constant of 5000 kcal/mol and a cutoff of 1 nm were applied to the AuNP beads in order to maintain the rigidity of the nanoparticle structure. The total mass of the AuNP is partitioned among the gold beads.

RESULTS AND DISCUSSION

The results obtained by coarse-grained molecular dynamics simulations of different amounts of insulins and fibrinogens interacting with a citrated-coated AuNP of core diameter 5 nm are described in the following in terms of corona formation and composition, protein binding sites, structural changes upon binding, competitive proteins adsorption, and multiple NP binding.

Insulin and fibrinogen are among the most abundant proteins in the plasma and show very different structural characteristics.

Insulin is a small protein, which promotes the adsorption of glucose to skeletal muscles, and it is responsible for lipid storage in fat tissue. It is a dimer made by two chains (A and B), respectively, of 21 and 30 amino acids, linked via two disulfide bonds with a compact round-shape tertiary structure and a molecular weight of 5.808 kDa.[24]

Fibrinogen is a rod-shaped protein, converted by thrombin into fibrin during the blood coagulation process. It has a molecular weight of 340 kDa and comprises three different polypeptide chains (α, β, and γ), arranged as a dimer. The elongated structure is approximately 45 nm long, and the diameter ranges from 1.7 to 4.55 nm.[23]

Corona Formation. In the first series of computational simulations, the formation of the corona has been investigated by varying the total number of insulin proteins (10, 20, 34, 50, 70, and 100) in the simulation box.

The number of proteins absorbed as a function of time for different protein concentrations is reported in Figure 1a. As expected, the number of absorbed insulins depends on the protein concentration considered. The maximum adsorption capacity of the citrate-coated AuNP with an extended diameter of 5.7 nm is 20, and it is reached after 40 ns, when 70 and 100 proteins are included in the simulation box.

In all cases, the corona is composed by a single layer of proteins (see Figure 1b, and Figure S1 in SI). In fact, at variance with the results obtained for other proteins such us ubiquitin,[13] only a limited tendency for aggregation of insulin proteins is highlighted in this study. The formation of a few dimers with a lifetime ranging from 1 to 3.5 ns is observed only occasionally, and in simulations with 100 insulins, two clusters made of three insulins, linked by a citrate molecule, are found.

The results of the series of computational simulations carried out with the fibrinogen proteins show that the maximum number of proteins that can bind to the citrate-coated AuNP is 3. Moreover, the probability of finding 1 or 3 proteins interacting contemporaneously with the AuNP is similar, i.e., 43%, and 37.5%, respectively. This unexpected result (fibrinogen is 45 nm long, i.e., 10 times the AuNP diameter)

DOI: 10.1021/acs.jpcc.5b05796
J. Phys. Chem. C 2015, 119, 22172−22180

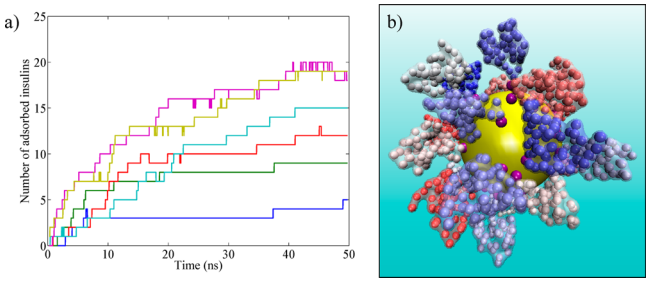

Figure 1. (a) Moving average of the number of insulin proteins bound to the citrate-coated AuNP during the computational simulation for different protein concentrations: 10 insulins in blue, 20 in green, 34 in red, 50 in cyan, 70 in purple, and 100 in brown. The data reported are relative to a single MD run chosen from a representative simulation. The moving average is performed over 25 time-steps in order to smooth out short-term fluctuations. (b) Snapshot of the protein corona around the citrate-coated AuNP made by 20 insulins. The snapshot has been taken from the computational simulation with 70 insulins at 45 ns; the insulins noninteracting with the AuNP are omitted for clarity reason. The coarse-grained models of the proteins are represented with different colors; citrates are represented in purple.

is due to the binding modalities of fibrinogen, and will be described in detail in paragraph 2.2.

Several numerical methods for the estimation of the adsorption capacity of a nanoparticle of given size have been published;[4,37,38] they mainly differ in the approximations made to consider the protein size and shape (see paragraph S.3 in SI for details).

Table 1 lists the results obtained with the methods of Calzolai et al.,[37] Dell'Orco et al.,[4] and Wang et al.,[38] together with the results obtained from the computational simulations carried out in this work.

Table 1. Maximum Number of Proteins That Can Bind to a Gold Nanoparticle (N_{max}) with a Gold Core Diameter of 5 nm[a]

	N_{max}			
	Calzolai[37]	Wang[38]	Dell'Orco[4]	this work
insulin	12	25	36	20
fibrinogen	1 (1.4)	1 (0.7)	7 (6.7)	3

[a]Calculated according to different numerical methods, and from the computational simulations carried out in this work for insulins and fibrinogens. The values $R_{protein}$(insulin) = 1.25 nm, $R_{protein}$(fibrinogen) = 8 nm, R_{gyra}(insulin) = 0.995 nm, and R_{gyra}(fibrinogen) = 5.97 nm have been used to compute data listed in the first three columns.

From the analysis of the data, the limitations of the approximation at the basis of the numerical methods considered are evident. In fact, good agreement with the results of the computational simulations is obtained only for insulins in the case of the method of Wang et al.,[38] which takes into account the radius of gyration of the protein.

The marked discrepancy with the number of adsorbed fibrinogens computed with the method of Dell'Orco et al.[4] is mainly due to the crude approximation of the protein shape to a sphere of radius 8 nm, and to the differences in the dimension of the NP considered (35 nm in ref 4).

Protein Conformational Changes upon Binding. The Ramachandran plots reported in Figure 2 show that the binding of the proteins to the citrate-coated AuNP induces a degree of disorder in their three-dimensional structure, although the overall conformation of both proteins is maintained.

The insulin protein (Figure 2a) shows a decrease in both the α-helix and β-sheets content upon binding with respect to the X-ray structure. However, this conformational change seems to be due not to the citrate-coated AuNP but to the dynamics of the protein at room temperature, since it is also observed in solution (NMR structure, pdb code 1HLS[39]). In fact, the percentages of α-helices and β-sheets content are 40.9 ± 10.2 and 2.1 ± 6.4 in the MD simulation, 47 and 0 in the NMR structure, 48.9 and 10.6 in the X-ray (4EWZ[24]) structure, respectively.

The Ramachandran plot of fibrinogen reported in Figure 2b shows differences in the secondary structure elements with respect to the starting configuration (crystal structures 3GHG:[23] blue stars) of the fibrinogen. However, on average, the variation in the α-helices and β-sheets content is on the order of the 2% and 3%, respectively.

These findings are in agreement with circular dichroism (CD) and fluorescence observations on the interaction between gold NPs of different diameters and common blood proteins: in general, small NPs better retain native-like protein structure and function in comparison with larger NPs.[40]

Protein Binding Site. The protein binding site can be identified by the analysis of the contact probability of each amino acid residue with the surface of the citrate-coated AuNP. The results for the insulin proteins are reported in Figure 3.

As demonstrated in a previous study on the interaction between ubiquitins and AuNPs of different sizes,[13] the area of the protein more suitable for the interaction is characterized by

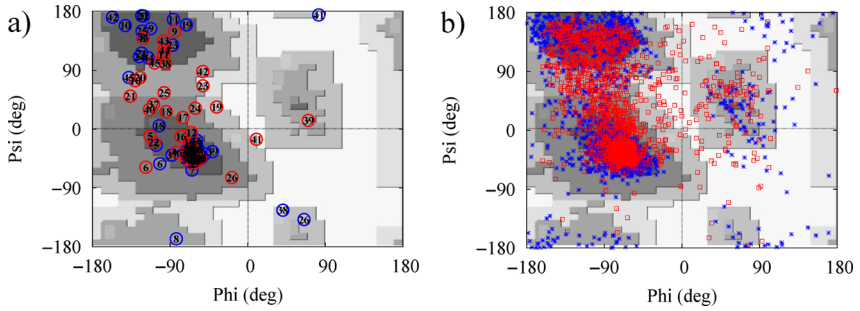

Figure 2. Ramachandran plot of (a) insulin and (b) fibrinogen. In blue, data from the X-ray structure, and in red, the data obtained, from the computational simulations, as mean of the dihedral angles computed on the adsorbed proteins. In part b, the numbers refer to the dihedral angle involved, while in part a labels are omitted for clarity.

DOI: 10.1021/acs.jpcc.5b05796
J. Phys. Chem. C 2015, 119, 22172−22180

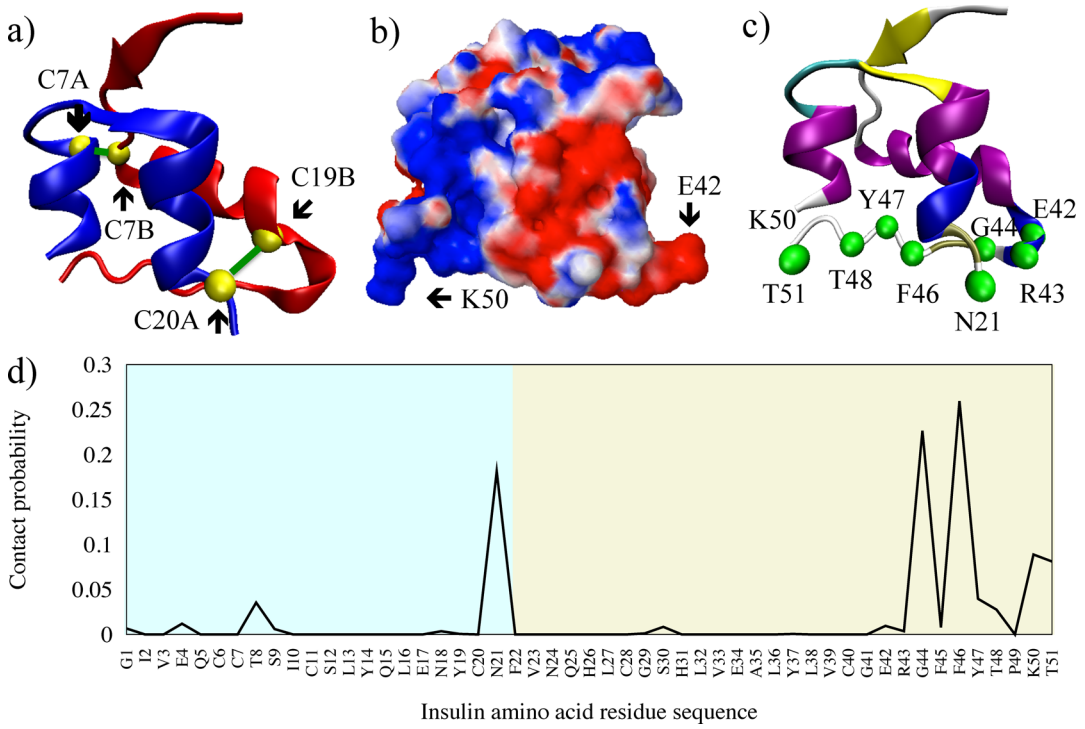

Figure 3. (a) Cartoon representation of the CG model of insulin (PDB ID: 4EWZ): chain A is colored in red, and chain B is in blue. Amino acids forming disulfide bonds are highlighted in yellow. (b) Electrostatic potential surface of insulin (atomistic level) where red areas represent negative potential and blue areas represent positive potential. (c) Cartoon representation of the CG model of insulin colored according to its secondary structure. Green beads represent the residues with high contact probability. (d) Contact probability of insulin amino acid residues with the citrate-coated AuNP surface: cyan area represents the chain A, and the beige area is chain B. A bead is considered to be in contact with the AuNP if its mean contact probability is greater than 0.001.

the presence of both positive and negative charges that can interact, respectively, with citrates and gold beads of the AuNP.

The electrostatic potential surface of insulin (reported in Figure 3b) shows that the region in the last half of the B chain (represented in red in Figure 3a) possesses this characteristic. In particular, the most significant contacts with the positive gold charged beads are made by E42 and the C-terminal of chain A (N21), whereas R43 and K50 interact with the negative citrates beads bonded to the AuNP (Figure 3d).

These residues are spatially close together, (Figure 3c) and define a specific contact probability area in line with the experimental results of SERS evaluation of the insulin−AuNP interactions, which showed that many functional groups, predominantly the carboxy groups, participate in bonding to the surface.[15]

The interaction established by these amino acid residues with the citrate-coated AuNP appears to be independent from the number of insulins considered in the computational simulations (and from the number of bound protein), as shown by the analysis of the binding energy per protein ($E_{binding}$), computed according to eq 8, and listed in Table 2. Indeed, while cooperative binding was observed experimentally for absorption of insulin to 100 nm NPs, little influence was observed on subsequent adsorption events to smaller nanoparticles (5 nm).[40]

Visual inspection of the trajectories reveals that the orientation of the insulins in an upright position on the AuNP surface with the N-terminal of the second chain upward is maintained in all the computational simulations, and the variation in the binding energies depends mainly on the

Table 2. Binding Energies as a Function of the Concentration of Adsorbed Proteins[a]

Insulins					
N_{tot} (N_{bound})	E_{tot}	$E_{citrates\text{-}AuNP}$	E_{prot}^{total}	$E_{binding}$	$\pm\Delta E_{binding}$
10 (4)	−1885.0	−1521.0	−321.3	−10.7	8.7
20 (9)	−2270.2	−1551.5	−633.0	−9.5	1.4
34 (12)	−2840.2	−1609.7	−1060.7	−14.1	1.3
50 (15)	−3363.0	−1584.7	−1542.7	−15.7	3.0
70 (20)	−3870.7	−1543.7	−2136.0	−9.82	2.2
100 (19)	−4866.7	−1611.0	−3090.5	−8.7	2.1
Fibrinogens					
N_{tot} (N_{bound})	E_{tot}	$E_{citrates\text{-}AuNP}$	$E_{prot\text{-}prot}^{interaction}$	$E_{binding}$	$\pm\Delta E_{binding}$
1 (1)	−5926	−1450	−3696	−780	17
2 (1)	−10 420	−1615	−7950	−855	35
4 (1)	−18 355	−1584	−16 065	−706	56
8 (3)	−33 448	−1589	−32 227		

[a] N_{tot} refers to the total number of proteins in simulation, while N_{bound} refers to the number of adsorbed proteins in simulation and $\pm\Delta E_{binding}$ is the absolute error of the binding energy. Energies are expressed in kcal/mol.

rearrangement of the citrates on the AuNP surface upon protein binding, that takes place in approximately 1−2 ns.

Nonspheroid or fibrous proteins, such as fibrinogen (Figure 4a), can interact with a surface in a number of configurations (Figure 4c). Both side-on binding and end-on binding of fibrinogen to different substrates have been described in the literature.[41,42] The electrostatic potential surface of fibrinogen is much less polarized with respect to that of insulin, and shows small negative and positive areas disseminated over the whole

DOI: 10.1021/acs.jpcc.5b05796
J. Phys. Chem. C 2015, 119, 22172−22180

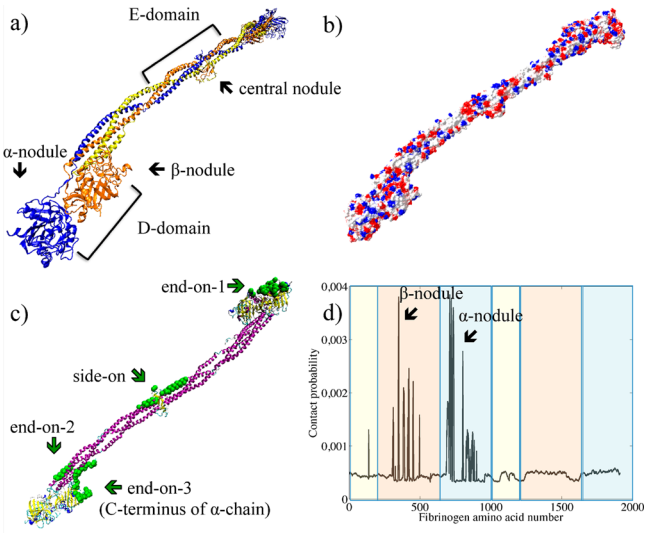

Figure 4. (a) Cartoon representation of the CG model of fibrinogen (PDB ID: 3GHG) where each nodule is labeled: the α-chain is colored in yellow, the β-chain is in orange, and the γ-chain is in blue. (b) Electrostatic potential surface of fibrinogen (atomistic level) where red areas represent negative potential and blue areas represent positive potential. (c) Cartoon representation the CG model of fibrinogen colored according to its secondary structures. Green beads represent the residues with high contact probability with the citrate-coated AuNP (binding regions). (d) Contact probability of fibrinogens with the AuNP surface. Different colored areas represent the three distinct fibrinogen chains: α-chain in yellow, β-chain in orange, and γ-chain in blue. A bead is considered to be in contact with the AuNP if its mean contact probability is greater than 0.0007.

molecule, (Figure 4b). In general, the molecular surface in the region comprising the boundary between the α-nodule and the β-nodule seems to possess the best characteristics required for the interaction with the citrate-coated AuNP. In fact, the most probable contacts are established with amino acid residues belonging to the α- and β-nodules (end-on-1 configuration), as highlighted in Figure 4c,d. However, with the binding being less specific with respect to the insulin protein, the overall contact probability is lower.

In the computational simulations carried out with 8 fibrinogens, three fibrinogens are interacting contemporaneously with the AuNP. Differences in the contact areas of each fibrinogen can be appreciated among the three molecules. Besides the area between the α- and β-nodules described formerly (end-on configuration, named end-on-1 in Figure 4c), the ending part of the β-nodule (end-on-2 in Figure 4c) and the region between the β-nodule and the α-helix (end-on-3 in Figure 4c) are also involved in the interaction (Figure 4c).

An exception to this general interacting behavior mainly involving the β-nodule and surrounding regions is observed in the computational simulation with 4 fibrinogens. In this case, only one molecule interacts with the AuNP, and the interacting site is localized on the central nodule (side-on) (Figure 4c).

The energetic consequences of the different binding modes are described in Table 2. In the first two computational simulations, with 1 and 2 fibrinogens, respectively, the binding mode and kinetic are almost the same (end-on-1, Figure 4), and the binding energies differ mainly for the citrate rearrangement on the AuNP surface. The interaction of fibrinogen via its central nodule (side-on, Figure 4) is less favored. In the simulation with 3 bound fibrinogens, the computed binding energy (not reported in Table 2) is positive due to steric hindrance among the three proteins. However, visual inspection of the trajectories shows that the proteins remain persistently bound to the AuNP through the citrate molecule.

The results obtained for fibrinogens are in contrast with the experimental observations of little effect on competitive or cooperative fibrinogen binding to small nanoparticles (5 nm),[39] probably because the high curvature of the NP increases the deflection angle between adsorbed proteins, decreasing protein−protein interactions.[43]

Competitive Binding of Insulins and Fibrinogens. A number of computational simulations have been carried out with different amounts of insulin and fibrinogen proteins contemporaneously present in the simulation box in order to get some light into the mutual effect of the two proteins on their binding modalities. In particular, the relative concentrations of insulin/fibrinogen of 10:1, 20:2, 34:4 have been considered. The results obtained, listed in Table 3, show a competition of these two kinds of proteins for binding with the citrate-coated AuNP. The presence of fibrinogens in the computational simulation box significantly reduce the number of insulins, which bind the citrate-coated AuNP.

The dynamics of the interaction is explained in Figure 5. In the computational simulation concerning the 10:1 protein ratio (Figure 5a), two insulins adsorb before the binding of fibrinogen, which occurs at around 20 ns of the dynamic run. A rearrangement of the proteins on the citrate-coated AuNP surface allows a third insulin molecule to be adsorbed after ∼8 ns. The four proteins remain contemporaneously bound to the nanoparticle for ∼15 ns, and then a steric repulsion occurs between the fibrinogen and the first molecule of insulin bound, forcing the insulin dissociation. When the relative concentration of insulins and fibrinogens is 20:2 (Figure 5b), only one insulin adsorbs onto the AuNP surface after 30 ns of the computational simulation. At approximately 45 ns a fibrinogen approaches the AuNP through its α-helix coiled coil region, but electrostatic repulsions with the adsorbed insulin occur. Therefore, the fibrinogen moves away, whereas the insulin remains bound to the nanoparticle. In the computational simulation with 34 insulins and 4 fibrinogens (Figure 5c), up to three insulins adsorb on the AuNP surface after 20 ns. These remain absorbed for 40 ns, and then a fibrinogen approaches

Table 3. Number of Proteins Adsorbed on the AuNP When Both Proteins Are Present in the Computational Simulation Box

	Insulin						Fibrinogen			
N of proteins in the simulation box	10	20	34	50	70	100	1	2	4	8
N of proteins adsorbed (after 50 ns)	5	9	12	15	20	19	1	1	1	3
	Insulin + Fibrinogen									
N of proteins in the simulation box	10	+	1	20	+	2	34	+	4	
N of Proteins Adsorbed (after 50 ns)	3	+	1	1	+	0	2	+	0	

DOI: 10.1021/acs.jpcc.5b05796
J. Phys. Chem. C 2015, 119, 22172−22180

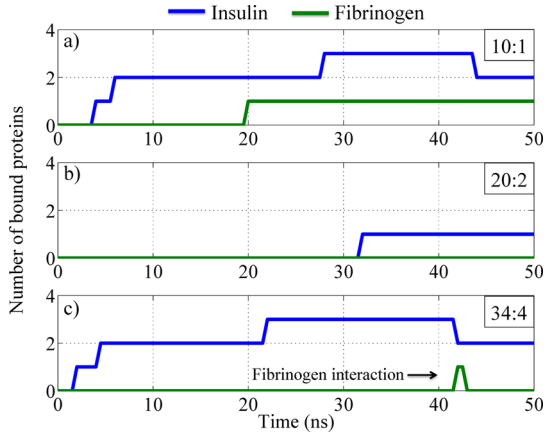

Figure 5. Number of proteins adsorbed on the citrate-coated AuNP as a function of time for the ratio insulin:fibrinogen of 10:1 (a), 20:2 (b), 34:4 (c). The blue line represents the number of insulins, and the green line the number of fibrinogens adsorbed on the AuNP during the computational simulation time. The data shown are relative to a single MD run chosen from a representative simulation.

the nanoparticle, interacts with an adsorbed insulin, and, being rejected, moves away provoking the dissociation of the insulin itself. After the first contact that provoked insulin desorption, insulin and fibrinogen move away from the nanoparticle independently.

The binding site of insulin in all the computational simulations with fibrinogens is the same as that reported in section describing the Contact Probability between Proteins and Citrate Coated AuNP, whereas the fibrinogen adsorbs mainly via the α-helix bundle close to the β-nodule. Insulin−fibrinogen interactions are not observed during the computational simulations.

Unfortunately, only the results of experimental determination of binding constants and the degree of cooperativity of single protein-NP[39] are available, whereas there is no other study that explores competitive or cooperative binding effects among different proteins.

Fibrinogen Interaction with Two AuNPs. The results of an experimental characterization of the molecular interaction between fibrinogen and negatively charged poly(acrylic acid)-coated AuNP of different size suggested that a single fibrinogen can bind up to two AuNPs with a core diameter of 5.7 nm.[18]

In this line, a molecular dynamics simulation of a single fibrinogen in a cubic box with two citrate-coated AuNPs with a 5 nm core diameter (extended-diameter citrates and AuNPs, is 5.7 nm) was carried out.

After 50 ns the two AuNPs bind to fibrinogen in two distinct ways, both localized in the ending nodes of the protein, in agreement with the two independent binding sites found by Deng et al.[18,44] on the basis of the measured Hill coefficient for the binding kinetics. As shown in Figure 6a, the first AuNP binds to the end surface of the α-nodule (end-on-1), and the second one to a region between the β-nodule and the α-chain (end-on-3). The first binding topology is the same observed as the most probable in the computational simulations carried out on 1 fibrinogen and 1 citrate-coated AuNP (Molecular Dynamics section). This is in agreement with the model proposed by Deng et al.,[18] based on the complementarity of the charge surfaces.[17] The second binding topology is the same observed in the computational simulations carried out on 2 and 8 fibrinogens and 1 citrate-coated AuNP (Molecular Dynamics section), and reproduces the binding of fibrinogen in the end-on configuration, usually evoked in the literature[17,18] when fibrinogen proteins bind large NPs (31.5 and 64.5 nm diameter).

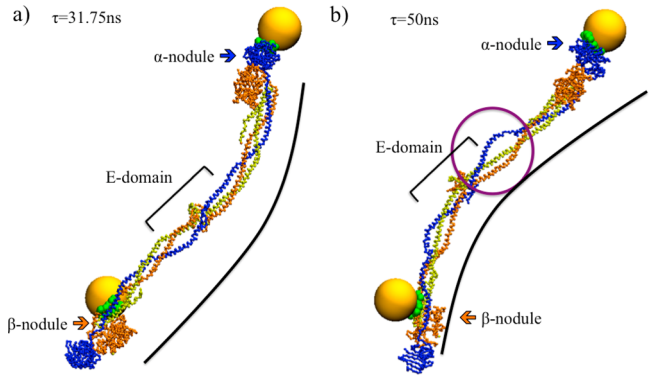

Figure 6. Snaphots of fibrinogen, at CG level, bound to two citrate-coated AuNPs taken at two different time-steps (31.75 and 50 ns) during the dynamics simulation. Green beads represent amino acids in contact with AuNPs. Black line shows the bending of fibrinogen along its principal axis. In part b, the purple circle shows the partial unfolding of the α-helix bundle near the central nodule.

It is worth noting that fibrinogen shows a propensity to bend along its principal axis when both the citrate-coated AuNPs are adsorbed. The bending originates at the central E-domain, as shown in Figure 6. Indeed, this is in line with the results of electron microscopy studies which depict the fibrinogen as a relatively flexible molecule: most molecules exhibit a θ value of 0.5°, while a few could bend as much as 90°, with the average angle of bend (θ) at the E-domain being 22°.[45]

The average angle of bending (θ) at the E-domain in the computational simulations carried out in this work is in agreement with the experimental value (~20°), and is almost the same before and after the binding of the 2 citrate-coated AuNP. However, the distribution of the θ angle values found during the computational simulations is narrower after AuNP adsorption, indicating a restricted mobility of the protein (see Figure S2 in SI).

Moreover, a partial unfolding of the α-helix bundle near the central nodule, highlighted with the purple circle in Figure 6b, is observed in the last part of the dynamics run. A loss of α-helical content upon bound 11-mercaptoundecanoic-acid-functionalized AuNPs of different sizes (5.6 and 14.2 nm diameter) was also highlighted by the results of far UV-CD spectroscopy.[44]

This phenomenon has relevant biological implication since it involves the exposition of a cryptic peptide located in the C-terminus of the fibrinogen γ-chain, which specifically interacts with the integrin receptor, Mac-1. Activation of this receptor increases the NF-κB signaling pathway, resulting in the release of inflammatory cytokines.[17]

CONCLUSIONS

The results of coarse-grained molecular dynamics simulations of insulins and fibrinogens interacting with citrate-coated AuNPs of 5 nm core diameter have furnished a detailed description of the process of corona formation.

Several effects have been explored: (a) the physicochemical characteristics and concentrations of each kind of protein with respect to NP adsorption; (b) the mutual competition of insulin and fibrinogen on the NP binding process; (c) the

DOI: 10.1021/acs.jpcc.5b05796
J. Phys. Chem. C 2015, 119, 22172−22180

binding of two NPs to fibrinogen; and (d) the protein conformational changes upon NP binding.

A maximum of 20 insulins can bind to citrate-coated AuNP of 5 nm core diameter, whereas only 3 fibrinogens are able to make persistent interactions with the AuNP, contemporaneously. In all cases, the corona is composed by a single layer of proteins, with only a limited tendency for aggregation being highlighted in this study.

The binding site for insulin is specific and constituted mainly by the C-terminal residues of the two dimer-chains, in line with experimental results; moreover, it is independent from the number of insulins considered in the computational simulations, as shown also by the computed binding energies per proteins. The binding site for fibrinogen is less specific; in general, it is located at the boundary between the α-nodule and the β-nodule (end-on-1 configuration). However, the ending part of the β-nodule (end-on-2), the region between the β-nodule and the α-helix (end-on-3), and the central nodule (side-on) are also involved in the interaction.

When insulins and fibrinogens are simulated together with the AuNP, a competitve binding process is observed. In particular, the number of adsorbed proteins shows a marked decrease with respect to the single protein simulations. The binding site of insulin in all the computational simulations with fibrinogens is the same as observed for insulin alone, whereas the fibrinogen adsorbs mainly via the α-helix bundle close to the β-nodule (end-on-3 binding mode). Insulin−fibrinogen interactions are not observed during the computational simulations.

In agreement with experimental observations, fibrinogen is able to accommodate two citrate-coated AuNPs in two independent binding sites localized in the ending nodes of the proteins.

The overall protein secondary structure is maintained upon binding to a single citrate-coated AuNP, but changes in helix and sheet content percentages are observed for both proteins. The propensity of fibrinogen to bend at the E-domain is interesting, as is the restricted mobility of the chain observed in the computational simulations carried out with two AuNPs. This triggers a partial unfolding of the α-helix bundle near the central nodule. Since the conformational state of fibrinogen is critical to leukocyte activation, this phenomenon may provide a molecular level understanding of the inflammatory response to nanoparticles.

■ ASSOCIATED CONTENT

Supporting Information

The Supporting Information is available free of charge on the ACS Publications website at DOI: 10.1021/acs.jpcc.5b05796.

Force-field parameters, number of bound insulins, AuNP adsorption capacity, and fibrinogen bending angle (PDF)

■ AUTHOR INFORMATION

Corresponding Author

*Phone: +39 059 2058 555. E-mail: mariacristina.menziani@unimore.it.

Notes

The authors declare no competing financial interest.

■ ACKNOWLEDGMENTS

This work was supported by the Italian Ministero dell'Istruzione, dell'Università e della Ricerca (MIUR) through the "Programma di ricerca di rilevante interesse nazionale" (PRIN) Grant 2010C4R8M8_002 entitled "Nanoscale Functional Organization of (bio)Molecules and Hybrids for targeted Application in Sensing, Medicine and Biotechnology" and the "Futuro in Ricerca" (FIRB) Grant RBFR1248UI 002 entitled "Novel Multiscale Theorethical/Computational Strategies for the Design of Photo and Thermo Responsive Hybrid Organic-Inorganic Components for Nanoelectronic Circuits".

■ REFERENCES

(1) Rahman, M.; Laurent, S.; Tawil, N.; Yahia, L.; Mahmoudi, M. *Protein-Nanoparticle Interactions*; Springer Series in Biophysics; Springer: Berlin, 2013; Vol. *15*.

(2) Mahmoudi, M.; Lynch, I.; Ejtehadi, M. R.; Monopoli, M. P.; Bombelli, F. B.; Laurent, S. Protein−Nanoparticle Interactions: Opportunities and Challenges. *Chem. Rev.* **2011**, *111*, 5610−5637.

(3) Vroman, L. Effect of Adsorbed Proteins on the Wettability of Hydrophilic and Hydrophobic Solids. *Nature* **1962**, *196*, 476−477.

(4) Dell'Orco, D.; Lundqvist, M.; Oslakovic, C.; Cedervall, T.; Linse, S. Modeling the Time Evolution of the Nanoparticle-Protein Corona in a Body Fluid. *PLoS One* **2010**, *5*, e10949.

(5) Monopoli, M. P.; Åberg, C.; Salvati, A.; Dawson, K. A. Biomolecular Coronas Provide the Biological Identity of Nanosized Materials. *Nat. Nanotechnol.* **2012**, *7*, 779−786.

(6) Wang, P.; Wang, X.; Wang, L.; Hou, X.; Liu, W.; Chen, C. Interaction of Gold Nanoparticles with Proteins and Cells. *Sci. Technol. Adv. Mater.* **2015**, *16*, 034610.

(7) del Pino, P.; Pelaz, B.; Zhang, Q.; Maffre, P.; Nienhaus, G. U.; Parak, W. J. Protein Corona Formation around Nanoparticles − from the Past to the Future. *Mater. Horiz.* **2014**, *1*, 301.

(8) Treuel, L.; Eslahian, K. A.; Docter, D.; Lang, T.; Zellner, R.; Nienhaus, K.; Nienhaus, G. U.; Stauber, R. H.; Maskos, M. Physicochemical Characterization of Nanoparticles and Their Behavior in the Biological Environment. *Phys. Chem. Chem. Phys.* **2014**, *16*, 15053−15067.

(9) Casals, E.; Pfaller, T.; Duschl, A.; Oostingh, G. J.; Puntes, V. Time Evolution of the Nanoparticle Protein Corona. *ACS Nano* **2010**, *4*, 3623−3632.

(10) Shemetov, A. A.; Nabiev, I.; Sukhanova, A. Molecular Interaction of Proteins and Peptides with Nanoparticles. *ACS Nano* **2012**, *6*, 4585−4602.

(11) Cukalevski, R.; Lundqvist, M.; Oslakovic, C.; Dahlbäck, B.; Linse, S.; Cedervall, T. Structural Changes in Apolipoproteins Bound to Nanoparticles. *Langmuir* **2011**, *27*, 14360−14369.

(12) Marino, V.; Astegno, A.; Pedroni, M.; Piccinelli, F.; Dell'Orco, D. Nanodevice-Induced Conformational and Functional Changes in a Prototypical Calcium Sensor Protein. *Nanoscale* **2014**, *6*, 412−423.

(13) Tavanti, F.; Pedone, A.; Menziani, M. C. A Closer Look into the Ubiquitin Corona on Gold Nanoparticles by Computational Studies. *New J. Chem.* **2015**, *39*, 2474−2482.

(14) Walkey, C. D.; Chan, W. C. W. Understanding and Controlling the Interaction of Nanomaterials with Proteins in a Physiological Environment. *Chem. Soc. Rev.* **2012**, *41*, 2780−2799.

(15) Grass, S.; Treuel, L. Mechanistic Aspects of Protein Corona Formation: Insulin Adsorption onto Gold Nanoparticle Surfaces. *J. Nanopart. Res.* **2014**, *16*, 2254.

(16) Chanana, M.; Correa-Duarte, M. A.; Liz-Marzán, L. M. Insulin-Coated Gold Nanoparticles: A Plasmonic Device for Studying Metal−Protein Interactions. *Small* **2011**, *7*, 2650−2660.

(17) Deng, Z. J.; Liang, M.; Monteiro, M.; Toth, I.; Minchin, R. F. Nanoparticle-Induced Unfolding of Fibrinogen Promotes Mac-1 Receptor Activation and Inflammation. *Nat. Nanotechnol.* **2011**, *6*, 39−44.

(18) Deng, Z. J.; Liang, M.; Toth, I.; Monteiro, M. J.; Minchin, R. F. Molecular Interaction of Poly(acrylic Acid) Gold Nanoparticles with Human Fibrinogen. *ACS Nano* **2012**, *6*, 8962−8969.

DOI: 10.1021/acs.jpcc.5b05796
J. Phys. Chem. C 2015, 119, 22172−22180

(19) Zhao, A. S.; Zhou, S.; Wang, Y.; Chen, J.; Ye, C. R.; Huang, N. Molecular Interaction of Fibrinogen with Thermally Modified Titanium Dioxide Nanoparticles. *RSC Adv.* **2014**, *4*, 40428−40434.
(20) Joshi, H. M.; Bhumkar, D. R.; Joshi, K.; Pokharkar, V.; Sastry, M. Gold Nanoparticles as Carriers for Efficient Transmucosal Insulin Delivery. *Langmuir* **2006**, *22*, 300−305.
(21) Marsaglia, G. Choosing a Point from the Surface of a Sphere. *Ann. Math. Stat.* **1972**, *43*, 645−646.
(22) Cook, J. M. Rational Formulae for the Production of a Spherically Symmetric Probability Distribution. *Math. Comput.* **1957**, *11*, 81−82.
(23) Kollman, J. M.; Pandi, L.; Sawaya, M. R.; Riley, M.; Doolittle, R. F. Crystal Structure of Human Fibrinogen. *Biochemistry* **2009**, *48*, 3877−3886.
(24) FáVero-Retto, M. P.; Palmieri, L. C.; Souza, T. A. C. B.; Almeida, F. C. L.; Lima, L. M. T. R. Structural Meta-Analysis of Regular Human Insulin in Pharmaceutical Formulations. *Eur. J. Pharm. Biopharm.* **2013**, *85*, 1112−1121.
(25) Tavanti, F.; Tozzini, V. A Multi-Scale−Multi-Stable Model for the Rhodopsin Photocycle. *Molecules* **2014**, *19*, 14961−14978.
(26) Clementi, C.; Nymeyer, H.; Onuchic, J. N. Topological and Energetic Factors: What Determines the Structural Details of the Transition State Ensemble and "en-Route" Intermediates for Protein Folding? An Investigation for Small Globular Proteins. *J. Mol. Biol.* **2000**, *298*, 937−953.
(27) Hills, R. D.; Brooks, C. L. Insights from Coarse-Grained Gō Models for Protein Folding and Dynamics. *Int. J. Mol. Sci.* **2009**, *10*, 889−905.
(28) Pincus, D. L.; Cho, S. S.; Hyeon, C.; Thirumalai, D. Minimal Models for Proteins and RNA: From Folding to Function. 2008, arXiv:0808.3099. *Cond-Mat Q-Bio*, http://arxiv.org/abs/0808.3099.
(29) Ding, F.; Radic, S.; Chen, R.; Chen, P.; Geitner, N. K.; Brown, J. M.; Ke, P. C. Direct Observation of a Single Nanoparticle−ubiquitin Corona Formation. *Nanoscale* **2013**, *5*, 9162−9169.
(30) Li, R.; Chen, R.; Chen, P.; Wen, Y.; Ke, P. C.; Cho, S. S. Computational and Experimental Characterizations of Silver Nanoparticle−Apolipoprotein Biocorona. *J. Phys. Chem. B* **2013**, *117*, 13451−13456.
(31) Giri, K.; Shameer, K.; Zimmermann, M. T.; Saha, S.; Chakraborty, P. K.; Sharma, A.; Arvizo, R. R.; Madden, B. J.; Mccormick, D. J.; Kocher, P.-J. A.; et al. Understanding Protein−Nanoparticle Interaction: A New Gateway to Disease Therapeutics. *Bioconjugate Chem.* **2014**, *25*, 1078−1090.
(32) Lin, W.; Insley, T.; Tuttle, M. D.; Zhu, L.; Berthold, D. A.; Král, P.; Rienstra, C. M.; Murphy, C. J. Control of Protein Orientation on Gold Nanoparticles. *J. Phys. Chem. C* **2015**, *119*, 21035.
(33) Smith, W.; Forester, T. R. DL_POLY_2.0: A General-Purpose Parallel Molecular Dynamics Simulation Package. *J. Mol. Graphics* **1996**, *14*, 136−141.
(34) Johansson, M. U.; Zoete, V.; Michielin, O.; Guex, N. Defining and Searching for Structural Motifs Using DeepView/Swiss-PdbViewer. *BMC Bioinf.* **2012**, *13*, 173.
(35) Humphrey, W.; Dalke, A.; Schulten, K. VMD: Visual Molecular Dynamics. *J. Mol. Graphics* **1996**, *14*, 33−3828.
(36) McWilliam, H.; Li, W.; Uludag, M.; Squizzato, S.; Park, Y. M.; Buso, N.; Cowley, A. P.; Lopez, R. Analysis Tool Web Services from the EMBL-EBI. *Nucleic Acids Res.* **2013**, *41*, W597−W600.
(37) Calzolai, L.; Franchini, F.; Gilliland, D.; Rossi, F. Protein−Nanoparticle Interaction: Identification of the Ubiquitin−Gold Nanoparticle Interaction Site. *Nano Lett.* **2010**, *10*, 3101−3105.
(38) Wang, A.; Vangala, K.; Vo, T.; Zhang, D.; Fitzkee, N. C. A Three-Step Model for Protein−Gold Nanoparticle Adsorption. *J. Phys. Chem. C* **2014**, *118*, 8134−8142.
(39) Ludvigsen, S.; Roy, M.; Thøgersen, H.; Kaarsholm, N. C. High-Resolution Structure of an Engineered Biologically Potent Insulin Monomer, B16 Tyr– > His, as Determined by Nuclear Magnetic Resonance Spectroscopy. *Biochemistry* **1994**, *33*, 7998−8006.
(40) Lacerda, S. H. D. P.; Park, J. J.; Meuse, C.; Pristinski, D.; Becker, M. L.; Karim, A.; Douglas, J. F. Interaction of Gold Nanoparticles with Common Human Blood Proteins. *ACS Nano* **2010**, *4*, 365−379.
(41) Adamczyk, Z.; Barbasz, J.; Cieśla, M. Mechanisms of Fibrinogen Adsorption at Solid Substrates. *Langmuir* **2011**, *27*, 6868−6878.
(42) Riedel, T.; Suttnar, J.; Brynda, E.; Houska, M.; Medved, L.; Dyr, J. E. Fibrinopeptides A and B Release in the Process of Surface Fibrin Formation. *Blood* **2011**, *117*, 1700−1706.
(43) Hill, H. D.; Muillstone, J. E.; Banholzer, M. J.; Mirkin, C. A. The Role Radius of Curvature Plays in Thiolated Oligonucleotide Loading on Gold Nanoparticles. *ACS Nano* **2009**, *3*, 418−424.
(44) Deng, J.; Sun, M.; Zhu, J.; Gao, C. Molecular Interactions of Different Size AuNP−COOH Nanoparticles with Human Fibrinogen. *Nanoscale* **2013**, *5*, 8130−8137.
(45) Beijbom, L.; Larsson, U.; Kavéus, U.; Hebert, H. Structure Analysis of Fibrinogen by Electron Microscopy and Image Processing. *J. Ultrastruct. Mol. Struct. Res.* **1988**, *98*, 312−319.

DOI: 10.1021/acs.jpcc.5b05796
J. Phys. Chem. C 2015, 119, 22172−22180